International Journal of Biological Macromolecules 254 (2024) 128101

Contents lists available at ScienceDirect

International Journal of Biological Macromolecules

journal homepage: www.elsevier.com/locate/ijbiomac

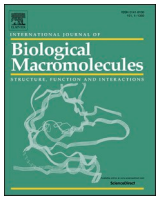

Hyaluronic acid/tannic acid films for wound healing application

Marcin Wekwejt [a], Marcin Małek [b], Anna Ronowska [c], Anna Michno [c], Anna Pałubicka [d], Lidia Zasada [e], Agnieszka Klimek [f], Beata Kaczmarek-Szczepańska [e,*]

[a] Department of Biomaterials Technology, Faculty of Mechanical Engineering and Ship Technology, Gdańsk University of Technology, Gabriela Narutowicza 11/12, 80-229 Gdańsk, Poland
[b] Faculty of Civil Engineering and Geodesy, Military University of Technology, ul. Gen. Sylwestra Kaliskiego 2, 00-908 Warsaw, Poland
[c] Department of Laboratory Medicine, Medical University of Gdańsk, Marii Skłodowskiej-Curie 3a, 80-210 Gdańsk, Poland
[d] Department of Laboratory Diagnostics and Microbiology with Blood Bank, Specialist Hospital in Kościerzyna, Alojzego Piechowskiego 36, 83-400 Kościerzyna, Poland
[e] Department of Biomaterials and Cosmetics Chemistry, Faculty of Chemistry, Nicolaus Copernicus University in Torun, Gagarina 7, 87-100 Toruń, Poland
[f] Faculty of Mechanical Engineering, Military University of Technology, ul. Gen. Sylwestra Kaliskiego 2, 00-908 Warsaw, Poland

ARTICLE INFO

Keywords:
Hyaluronic acid
Tannic acid
Thin films
Hemocompatibility
Cytocompatibility
Irritation effect

ABSTRACT

In this study, thin films based on hyaluronic acid (HA) with tannic acid (TA) were investigated in three different weight ratios (80HA/20TA, 50HA/50TA, 20HA/80TA) for their application as materials for wound healing. Surface free energy, as well as their roughness, mechanical properties, water vapor permeability rate, and antioxidant activity were determined. Moreover, their compatibility with blood and osteoblast cells was investigated. The irritation effect caused by hyaluronic acid/tannic acid films was also considered with the use of are constructed human epidermis model. The irritation effect for hyaluronic acid/tannic acid films by the in vitro method was also studied. The low surface free energy, surface roughness, and antioxidant activity presented by the obtained films were examined. All the tested compositions of hyaluronic acid/tannic acid films were hemocompatible, but only films based on 50HA/50TA were fully cytocompatible. Regarding the potential implantation, all the films except 80HA/20TA showed appropriate mechanical properties. The specimens did not exert the irritation effect during the studies involving reconstructed human epidermis.

1. Introduction

Biopolymers are compounds of natural origin [1] characterized as biocompatible and biodegradable [2], which attracts a significant scientific interest. Nevertheless, "pure" biopolymers do not meet the criteria required for materials applied as wound dressings [3] and their further modifications are necessary, e.g. by the addition of various compounds, the so-called cross-linkers [4] which form new bonds or interactions between functional groups present in polymer chains. Such modifications improve the stability of the materials and allow their employment as biocompatible coatings or layers [5].

Hyaluronic acid, an organic compound found in virtually all organisms, is a non-sulfate glycosaminoglycan (GAG) composed of repeating β (1- > 3) D-glucuronic acid disaccharides [6]. The polysaccharide of the glycosaminoglycan group occurs naturally as a component of the intracellular matrix in dermis [7–9] and is also present in the human body as a sodium salt (sodium hyaluronate). Hyaluronic acid may differ in a degree to which it is cross-linked, i.e. it may be of various densities and different levels of bonding to water molecules. As an extracellular matrix component, hyaluronic acid promotes cell proliferation, angiogenesis, and tissue regeneration (e.g. wound healing) [9–11]. Such properties allow the use of hyaluronic acid biomaterials mainly in cosmetic medicine (e.g. restoring skin volume), in ophthalmic surgery, and in the treatment of other degenerative joint diseases [12,13]. A less common hyaluronic acid application is connected to wound healing as the employment of polysaccharides to form hydrogel dressings is required in order to shorten wound healing time [14,15].

Tannins, which are represented by tannic acid, constitute a group of organic chemical compounds of natural origin. Tannic acid, composed of glucose and gallic acid molecules [16], presents antibacterial and antioxidant properties, as well as biocompatibility [17–20]. As evidenced, tannic acid supports skin regeneration, e.g. in the treatment of burns [21]. Moreover, tannic acid is an effective cross-linking agent for natural polymers such as hyaluronic acid [16], chitosan [22], collagen [23] and starch [24].

The aim of the study was to obtain and characterize novel materials

* Corresponding author.
E-mail address: beata.kaczmarek@umk.pl (B. Kaczmarek-Szczepańska).

https://doi.org/10.1016/j.ijbiomac.2023.128101
Received 4 May 2023; Received in revised form 10 November 2023; Accepted 13 November 2023
Available online 14 November 2023

based on hyaluronic acid/tannic acid in thin film form that were fabricated by solvent evaporation. The properties of the materials i.e. surface properties, mechanical parameters, water vapor permeation rate, and antioxidant activity were determined. Additionally, biocompatibility with blood and cells as well as the irritation effect of the studied films with the use of the reconstructed human epidermis test method were investigated according to OECD 439 "In Vitro Skin Irritation: Reconstructed Human Epidermis Test Method" norm to consider the obtained materials as safe for use as wound dressing.

2. Materials and methods

2.1. Materials

Hyaluronic acid (HA, Mv = 1.8×10^6 g/mol) and 2,2-Diphenyl-1-picrylhydrazyl were purchased from Sigma-Aldrich. Tannic acid (TA, $M_w = 1701.23$ g/mol) and acetic acid (98 %) were purchased from the ROTH company. MTT (3-(4,5-dimethylthiazol-2-yl)-2,5-diphenyltetrazolium bromide) and (*S*)-lactate: NAD + oxidireductase (lactate dehydrogenase, LDH, EC 1.1.1.27) assays, culture medium (Ham's F12 and Dulbecco's Modified Eagle's), geneticin disulfate salt (G418), fetal bovine serums (FBS) and Triton X-100 were purchased from the Merck company.

2.2. Film preparation

Hyaluronic acid and tannic acid were dissolved in 0.1 M acetic acid at 1 % concentration, separately. The solutions were mixed in three weight ratios (HA/TA):80/20, 50/50, and 20/80. Such mixtures were placed on the magnetic stirrer and mixed for 2 h. The final concentrations of the components in the mixtures were: 0.008 g/mL HA and 0.002 g/mL TA in the 80HA/20TA film (ratio 4:1); 0.005 g/mL HA and 0.005 g/mL TA in the 50HA/50TA (ratio 1:1), and 0.002 g/mL HA and 0.008 g/mL TA in the 20HA/80TA (ratio 1:4). All the mixtures were placed on the plastic holder (40 mL per 10 cm × 10 cm). The films were obtained by drying at room temperature in the air atmosphere for 48 h (Fig. 1). The films composed of pure hyaluronic or tannic acid could not be successfully fabricated after solvent evaporation for further testing as they were too brittle.

2.3. ATR-FTIR spectroscopy

Infrared spectra of the films were collected with a Nicolet iS5 (Thermo Fisher Scientific, Waltham, MA, USA) spectrophotometer with ID7 ATR equipment containing ZnSe crystal, at room temperature in the air atmosphere. The operating parameters were applied: 4 cm^{-1} resolution, 32 scans, and the range of wavenumbers 4000–550 cm^{-1}.

2.4. Surface free energy

The contact angles of two liquids (glycerin and diiodomethane) on the films were measured using a goniometer equipped with a drop shape analysis system (DSA 10 Control Unit, Krüss, Germany) at room temperature in an air atmosphere. Then, the values of the contact angle measurement for both liquids were used to calculate the surface free energy (IFT) and its polar (IFT (s,P)) and dispersive (IFT (s,D)) components using the Owens–Wendt method [25].

2.5. Atomic force microscopy (AFM)

The surface roughness was determined from the images obtained with the microscope equipped with a scanning probe of the NanoScope IIIa MultiMode Scanning Probe Microscope type (Veeco Metrology, Inc., Santa Barbara, CA, USA) which operated in a tapping mode at room temperature in an air atmosphere. Two parameters were calculated: the root-mean-square (Rq) roughness and the arithmetic mean (Ra) within the Nanoscope Analysis v6.11 software (Bruker Optoc GmbH, Ettlingen, Germany).

2.6. Mechanical properties

The mechanical properties of the films were determined by the nanoindentation technique with NanoTest™ Vantage equipment (Micro Materials, UK). The experiments were performed using a three-sided diamond and a pyramidal indenter (Berkovich indenter). The following parameters were set up: 200 mN maximum force, 20 s of the loading time, 15 s of the unloading time and 5 s of the holding time under maximum force. After each test, temperature drift was allowed for 10 s. The load-displacement curves were determined for each film ($n = 10$) and the hardness (H) and reduced Young's Modulus (Er) were calculated by the Oliver and Pharr method [26] using the integrated software.

2.7. Water vapor permeation rate (WVPR)

The water vapor permeation rate is the parameter that allows the determination of water permeation through a film. A known weight of dried anhydrous calcium chloride (m_0) as a desiccant was placed in a plastic container with a 5 cm diameter. The films were placed on top of the containers and sealed tightly [27]. After 3 days, the samples were weighed (m_t) and the changes in their weights were determined:

$$\text{the percentage weight gain of } CaCl_2 = \frac{m_t - m_0}{m_0} * 100\% \quad (1)$$

2.8. Water stability

Dry films with a known weight (m_0) were immersed in distilled water. After 1 and 24 h (m_t), the subjected samples were removed from

Fig. 1. Digital images of the obtained films A) 80HA/20TA, B) 50HA/50TA, C) 20HA/80TA.

the solution, gently dried with tissue paper, and weighed. The percentage of weight change was then calculated:

$$weight\ change = \frac{m_t - m_0}{m_0} * 100\% \quad (2)$$

2.9. DPPH radical scavenging assay

The antioxidant properties of the films were determined using the DPPH reagent (2,2-Diphenyl-1-picrylhydrazyl, free radical, 95 %; Alfa Aesar, Germany). Samples (1 cm × 1 cm) of each film were placed in a 24-well plate and filled with 2 mL of a DPPH solution (250 μM solution in methyl alcohol). They were left without exposure to light for 0.5 h. A spectrophotometric measurement was made at 517 nm (UV-1800, Shimadzu, Switzerland). The antioxidant activity was calculated from the formula:

$$RSA\% = \frac{Abs_{DPPH} - Abs_{PB}}{Abs_{DPPH}} * 100\% \quad (3)$$

where:

Abs_{DPPH} is the absorbance of the DPPH solution without contact with the material being tested

Abs_{PB} is the absorbance of the DPPH solution after contact with the material being tested

2.10. Hemo- and cyto-compatibility

The experiments on hemo- and cyto-compatibility of the films were conducted on human red blood cells (RBCs) and human osteoblasts cell line (hFOB 1.19, RRID: CVCL 3708; ATCC, USA). The number of cells was estimated with a Superior CE hemocytometer (Marienfeld, Lauda-Königshofen, Germany). To study the hemocompatibility, square samples of the films which were 5 mm in diameter and 0.13 (± 0.02) mm in thickness were examined. To check the cytocompatibility, round-shaped samples of 15 mm in diameter and the same thickness were used. Prior to the testing, all the specimens were sterilized by exposure to UV-light for 30 min. The results are presented in percentages relating to the relevant controls [28], while direct values are included as SFigs. 1 and 2 in Appendix.

RBCs were obtained from buffy coats highly contaminated with RBCs obtained as by-products of whole blood fractionations from the Regional Blood Centre in Gdańsk (Regional Blood Blank institutional permission M-073/17/JJ/11). Whole blood was collected from healthy volunteers in accordance with the Declaration of Helsinki under an approved Regional Bank Review Board Protocol in standard acid citrate dextrose solutions. RBCs were fractionated according to Blood Banks standards [29]. RBCs (3×10^9 cells/mL) were placed in 2 mL tubes containing films ($n = 4$) and incubated at 37 °C for up to 24 h. The remaining blood samples were centrifuged at 100 ×*g* at room temperature for 3 min to let the erythrocytes sediment, and supernatants were taken for further research. The hemolysis was assessed spectrophotometrically at a 540 nm wavelength with Ultrospect 3000pro spectrophotometer (Amersham-Pharmacia-Biotech, Cambridge, UK). RBCs treated with 2 % Triton were used as a positive control (i.e. 100 % hemolysis) and RBCs incubated without films as a negative control [26].

The hFOB cells were grown in 1:1 mixture of Ham's F12 Medium and Dulbecco's Modified Eagle's Medium (without phenol red), containing 1 mmol/L L-glutamine, 0.3 mg/mL genetin disulfate salt (G418) and 10 % fetal bovine serum at 37 °C in an atmosphere containing 5 % CO_2. Extracts of the films were used to study their cytocompatibility effect. Each film ($n = 4$) was immersed in 2 mL of the culture medium and conditioned for 24 h. The cells were seeded at a density of 12×10^3 cells on a 96-well plate and cultured for 24 h under standard conditions. The medium was further discharged and the conditioned medium was added for the next 72 h. The cell viability was evaluated after 72 h of culture using the MTT assay (3-(4,5-dimethylthiazol-2-yl)-2,5-diphenyltetrazolium bromide). The medium was changed for one supplemented with 0,06 mmol/L of MTT and incubated for another 4 h. The viable cells containing NAD(*P*)H-dependent oxidoreductase enzymes reduced the MTT to blue formazan. The absorbance was measured spectrophotometrically at 590 nm. The measured absorbance was proportional to the number of viable cells. The results are expressed as a % of non-treated control (TCP). Moreover, the LDH release assay was used to determine cell death by the assessment of LDH release from the dead cells. The supernatants from the hemocompatibility test and the culture medium from the cytocompatibility test were used for this study. The lactate dehydrogenase (LDH, fractional (*S*)-lactate:NAD+ oxidoreductase; LDH, EC 1.1.1.27) was surveyed by direct measurement of NADH oxidation at 340 nm. LDH data were expressed as a percentage of the total LDH released from the cells.

2.11. Antibacterial properties

The inhibition of bacterial growth was evaluated according to the McFarland standards [30] by measuring the turbidity of bacteria incubated together with films. Briefly, when the optical density of the bacterial suspension is 1.0 McFarland index (iMS), the number of bacteria is 3×10^8 CFU/mL. Before testing, the examined films ($n = 3$; 0.5 × 0.5 × 0.1 mm) were placed in 24-well plates and sterilized by UV-light exposure for 30 min. *Staphylococcus aureus* (ATCC 25923; USA) and *Escherichia coli* (ATCC 25922, USA) bacteria with an initial concentration of 0.5 iMS were suspended in Trypticase Soy Broth (Merck, Darmstadt, Germany) and then added to wells with the specimens (2 mL) and incubated at 36 °C. After each hour, their optical density was measured using the DensiChEK Plus (BioMerieux, Montreal, QC, Canada). Bacteria incubated without specimens were used as a negative control. The maximum measuring range of the device was 4 iMS.

2.12. Irritation effect

The films were tested according to the OECD 439 "In Vitro Skin Irritation: Reconstructed Human Epidermis Test Method" norm using the reconstructed human epidermis model (EpiDerm - Reconstructed Human Epidermis; Mattek In Vitro Life Science Laboratories, EpiDerm Frozen EPI-200 ver. 2.0). The reconstructed human epidermal model EpiDerm™ consists of normal human epidermal derived keratinocytes that have been cultured to form multi-layered, highly differentiated human tissue. It consists of an organized basal, spinous, granular and multilayer stratum corneum layer containing intercellular lamellar lipid layers.

The test involves the local exposure of the chemical under examination to the tissue surface for a specified period of time, which is followed by a cell viability test quantified using the MTT test. The MTT test enables the measurement of the activity of mitochondrial enzymes in the cell, which is directly proportional to the amount of reduced tetrazolium salt, and thus may be an indicator of cell viability.

2.13. Statistical analysis

The statistical analysis of the data was performed using the commercial software (SigmaPlot 14.0, Systat Software, San Jose, CA, USA). The Shapiro-Wilk test was used to assess the normal distribution of the data. All the results were calculated as mean ± standard deviations (SD) and statistically analyzed using the one-way analysis of variance (one-way ANOVA). Multiple comparisons versus the control group between the means were performed using the Bonferroni *t*-test with the statistical significance set at $p < 0.05$.

3. Results

3.1. ATR-FTIR spectroscopy

ATR-FTIR spectra of the studied films containing tannic acid as well as of the films containing solely hyaluronic acid without tannic acid addition (HA) are shown in Fig. 2. All the spectra show the peak at 1034 cm^{-1} attributed to C-O-C vibration, and the peaks at 1602 cm^{-1} attributed to the asymmetric bending of C═O groups in HA [31]. The spectrum of hyaluronic acid shows a peak at 1410 cm^{-1} attributed to the symmetric stretching of C═O groups in HA, however, it is not observed in the spectra of HA/TA films. The spectrum in the region of 1490–1286 cm^{-1} has been changed with the addition of tannic acid. The change is related to the coupled vibrations of the ring (C—C) and the carbonyl group (C═O), are formed together with the contribution from vibrations of the C—H and C–OH groups. Also, a peak at 1210 cm^{-1} is presented in the spectra of HA/TA characteristic for the phenol group [32,33].

3.2. Surface free energy

The surface free energy was determined by measuring the contact angle of the polar and the non-polar liquid placed on the film surface (Table 1). Surface free energy values determine the dangling bonds which control cell-material interactions. High surface free energy inhibits such interactions. The results showed that the increasing amount of tannic acid present in the film results in the decrease in surface free energy. The polar component also decreased with an increasing tannic acid content, as hyaluronic acid is highly hydrophilic. The opposite trend was observed for the dispersive component since films with the highest tannic acid content showed the lowest IFT (s,D) parameter.

3.3. Atomic force microscopy (AFM)

The roughness of the film influences the material properties. Table 2 shows the roughness parameters. The increasing amount of tannic acid results in the decrease in both roughness parameters. It suggests that the addition of tannic acid results in the changes in organization of the polymer chain of hyaluronic acid. Thereby, fewer functional groups are present on the films' surface (Fig. 3) and as a result, roughness decreases.

3.4. Mechanical properties

The mechanical properties of the films such as nanohardness and Young's Modulus (Fig. 4) were calculated based on the nanoindentation curves shown in Fig. 5. Each hysteresis plot of load-deformation consists of three characteristic segments: 1) loading with increasing the force to at certain value, 2) holding with maintaining the applied force and 3) unloading. Also, in all plots a slight deformation at the last stage is visible, which was related to the temperature drift. Different compositions of the film ingredients (HA/TA) significantly influenced the shape of nanoindentation curves as well as both of the tested parameters. The increase in TA content significantly improves mechanical resistance and increases Young's Modulus, while the opposite effect was observed for increasing the HA content. The meaningful increase in the depth of indentation was only noted for 80HA/20TA. The 50HA/50TA film had optimal mechanical properties, while the 20HA/80TA film had the best characteristics.

Table 1
The surface free energy (IFT(s)), its polar (IFT (s,P)) and dispersive (IFT (s,D)) components of the films based on hyaluronic acid and tannic acid ($n = 5$; * significantly different from 20HA/80TA — $p < 0.05$; # significantly different from 50HA/50TA — $p < 0.05$).

Specimen	IFT(s) [mJ/m^2]	IFT (s,P) [mJ/m^2]	IFT (s,D) [mJ/m^2]
80HA/20TA	54.25 ± 0.99*#	30.22 ± 0.50*#	24.03 ± 0.48*#
20HA/80TA	42.61 ± 1.21	15.41 ± 0.41	27.21 ± 0.81
50HA/50TA	44.17 ± 0.56	16.02 ± 0.24	28.15 ± 0.31

Table 2
Roughness parameters (Ra and Rq) of films ($n = 5$; * significantly different from 20HA/80TA — $p < 0.05$; # significantly different from 50HA/50TA — $p < 0.05$).

Specimen	Ra [nm]	Rq [nm]
80HA/20TA	3.45 ± 0.17#	4.21 ± 0.17#
20HA/80TA	2.92 ± 0.10	3.84 ± 0.09
50HA/50TA	2.97 ± 0.13*	3.88 ± 0.21*

3.5. Water vapor permeation rate (WVPR)

The water vapor permeation rate is at parameter that allows the determination of water permeation from atmosphere through a film. An increasing amount of tannic acid in the film results in the decrease in WVPR (Table 3). The film composed of 80HA/20TA has the highest ability to allow water to permeate through the material.

3.6. Water stability

The weight change of hyaluronic acid/tannic acid films in water can be considered as their stability in water. For each type of film, after 1 and 24 h of immersion in water, an increase in weight was observed. It suggests that each film has the ability to swell and that it does not degrade after 24 h. The experiment was not carried out for a longer period of time because the films dissolved. Films containing a higher

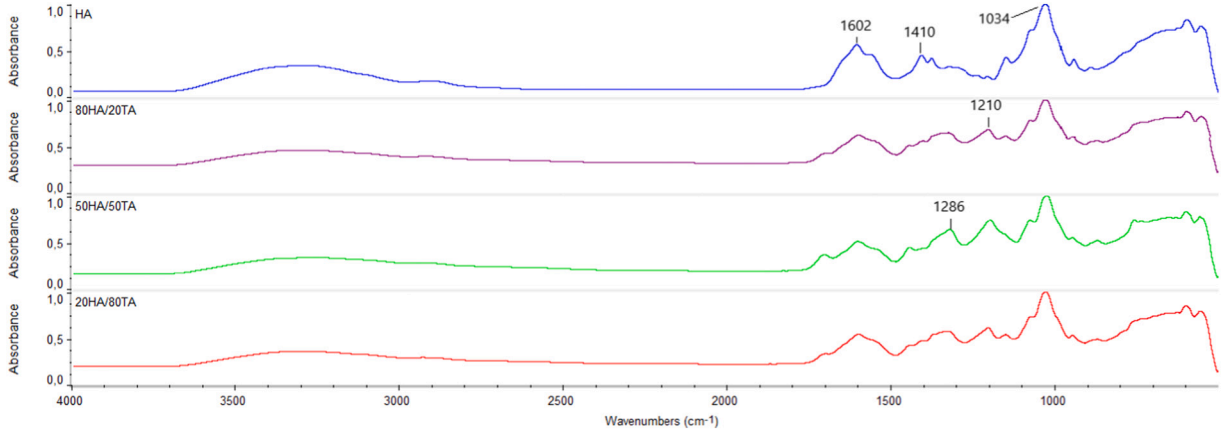

Fig. 2. The ATR-FTIR spectra of hyaluronic acid (HA), 80HA/20TA, 20HA/80TA, and 50HA/20TA.

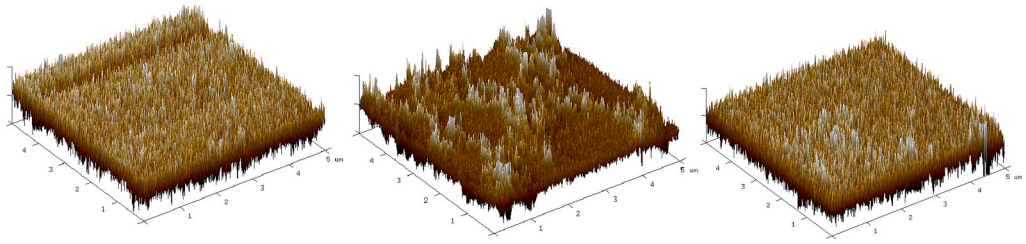

Fig. 3. The 3D images of surfaces of films 80HA/20TA, 20HA/80TA, 50HA/20TA, respectively.

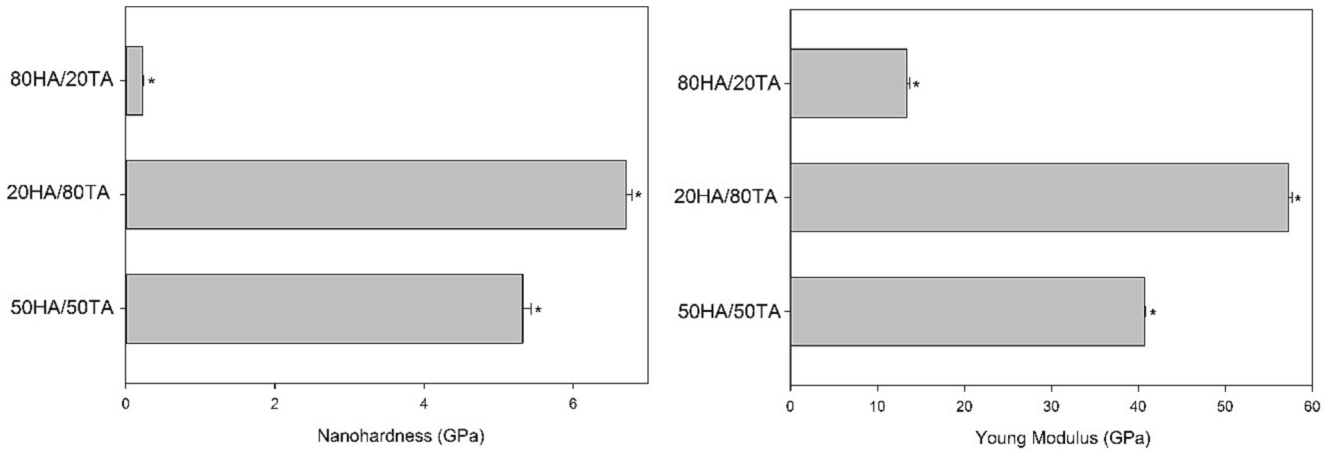

Fig. 4. Nanoindentation mechanical properties of the tested films ($n = 10$; data are expressed as the mean ± SD,* significantly different between groups ($p < 0.05$)).

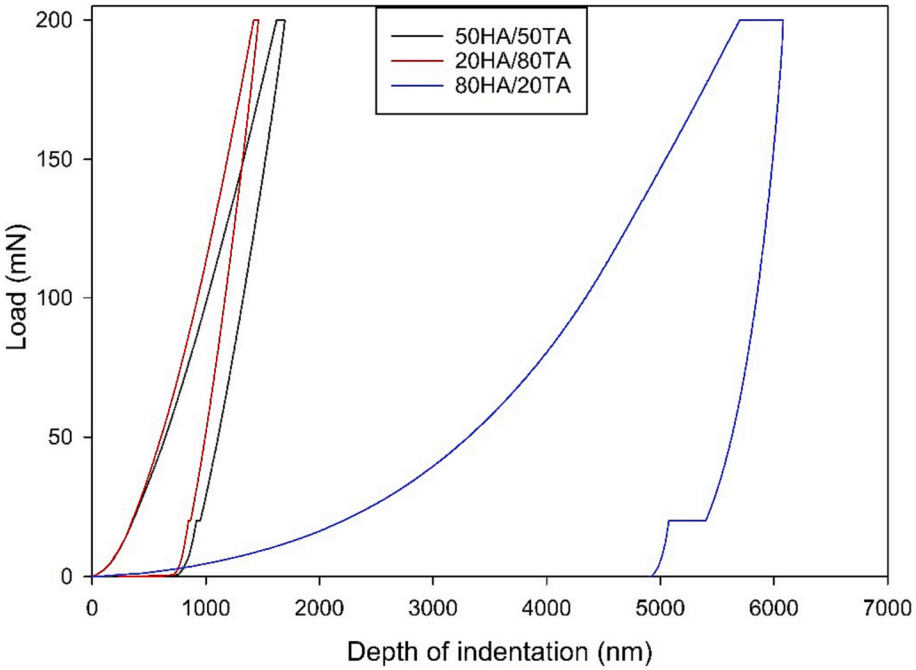

Fig. 5. Nanoindentation curves for the tested films (the presented plots are representative for ten indentation experiments).

concentration of HA showed higher swelling behavior than those with a lower HA content.

3.7. DPPH radical scavenging assay

The antioxidant properties were determined by the DPPH radical scavenging assay method (Table 3). All the tested films showed the positive radical scavenging activity (RSA); however, its value depends on the film composition. Tannic acid is well-known as a natural compound with antioxidant properties [17]. The increase in tannic acid content in the material results in the increase in RSA.

Table 3
The water vapor permeability rate recalculated to mg/cm^2/h units (WVPR), (n = 5; * significantly different from 20HA/80TA — $p < 0.05$; # significantly different from 50HA/50TA — $p < 0.05$).

Specimen	WVPR [mg/cm^2/h]	RSA [%]	Weight change in water [%]	
			1 h	24 h
80HA/20TA	0.1759 ± 0.0049*#	26.15 ± 0.21*#	570 ± 12*#	1040 ± 19*#
20HA/80TA	0.1415 ± 0.0061#	93.22 ± 1.05#	490 ± 11#	870 ± 10#
50HA/50TA	0.1621 ± 0.0092	85.78 ± 0.56	418 ± 15	822 ± 13

3.8. Hemo- and cyto-compatibility

The developed films did not have a negative effect on the human erythrocytes (Fig. 6B), which is confirmed by the low degree of hemolysis (below 0.5 %), and low release of LDH from the cells was comparable to the control conditions. While some of the tested films were cytostatic to hFOB 1.19 cells, 20HA/80TA and 80HA/20TA inhibited the cellular growth by ~50 %, but they were not cytotoxic because the LDH release was not elevated. In turn, 50HA/20TA was the most biocompatible one as it neither decreased the cellular growth nor increased the LDH release (Fig. 6A).

3.9. Antibacterial properties

All the developed films showed antibacterial properties against both *Staphylococcus aureus* and *Escherichia coli* and contributed to the slowdown in their growth in the broth (Fig. 7). In this study, it was observed that the 20HA/80TA films dissolved completely during the test, which may affect the collected results. The most effective inhibitory effects on *Staphylococcus aureus* (~10 %) were observed for the 50HA/50TA film, while on *Escherichia coli* (~14 %) - for the 20HA/80TA film.

3.10. Irritation effect

The irritation effect study confirms the safety of the specific materials in use when getting in contact with human skin. The mean tissue viability (expressed as % of NC negative control) above 50 % means that a polymer film does not present an irritation effect (Table 4). The obtained results showed that none of the films has any irritation effect. The %NC increases with an increase in the amount of hyaluronic acid.

4. Discussion

Hyaluronic acid is a well-known polysaccharide and a component of different types of biomaterials. It is biocompatible and safe to use in both external and internal applications. Hyaluronic acid may be combined with other natural compounds to enhance the material's properties and provide new properties. Tannic acid is a polyphenolic acid known as a good cross-linker for polysaccharides [34]. In this study, tannic acid was mixed with hyaluronic acid and the resulting thin films were obtained by solvent evaporation. ATR-FTIR spectra showed characteristic peaks of hyaluronic acid and a phenolic compound (tannic acid). Some changes can be observed due to the possible hydrogen bonding between the hydroxyl groups of TA and the hydrophilic groups of hyaluronic acid.

Surface free energy constitutes an important parameter when examining cell interactions with the surface and, at the same time, the materials' biocompatibility. The presence of tannic acid results in the decrease in surface free energy which may further cause the improvement of the cell-material interaction. There is yet another important parameter influencing the cell behavior, i.e. the surface roughness. The surface topography strongly modulated the cellular morphology, proliferation and phenotype expression. The surface roughness can be classified as nanoroughness (<100 nm), microroughness (100 nm–100 μm), or macroroughness (100 μm–1 mm) [35]. The surface roughness of the fabricated films based on hyaluronic acid/tannic acid was at the nanomater scale. Depending on a cell type, the nanoscale roughness may either improve or hamper the biofilm formation [36].

Mechanical properties are extremely important in terms of the application aspect. In our nanoindentation research, we found that the composition (i.e. percentage content of HA and TA) of films has a remarkable effect on both hardness and Young's Modulus. An increase in the TA content improves these properties, which is probably related to

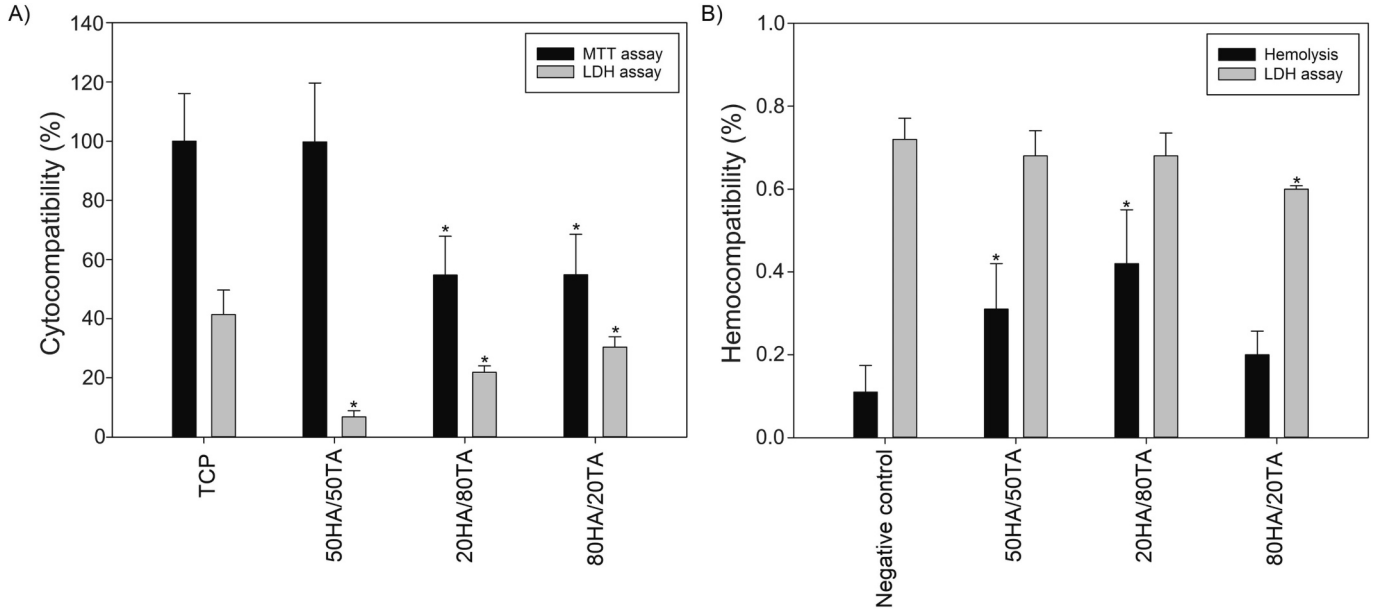

Fig. 6. The effect of the developed films on cytocompatibility of hFOB 1.19 cells (cell viability and lactate dehydrogenase release) after 72 h of culture and hemocompatibility of human erythrocytes (hemolysis rate and lactate dehydrogenase release) after 24 h exposure to films (n = 4, data are expressed as the mean ± SD,* significantly different from the respective controls ($p < 0.05$)).

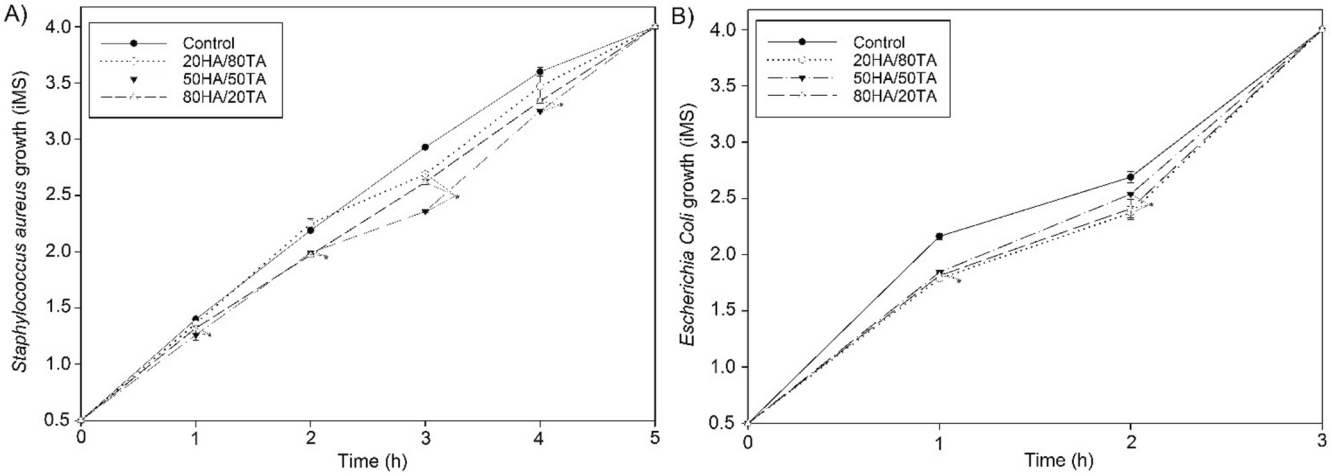

Fig. 7. Bacterial growth inhibition determined by McFarland standard values specifying the number of the selected bacteria during incubation with the tested films: A) *Staphylococcus aureus* and B) *Eschericha coli* ($n = 3$; data are expressed as the mean ± SD,* significantly different from control ($p < 0.05$)).

Table 4
The results of the irritation effect studies for films based on hyaluronic acid and tannic acid.

	Absolute value [OD]	SD [%]	Acceptance criterion	Result
Negative control – NC	1.456	7.62	OD ≥ 1 and OD ≤ 2.8 and SD ≤18 %	Normal
	Average tissue viability [% NC]	SD [%]	Acceptance criterion	Result
Positive control – PC	3.6	0.25	%NC < 20 % and SD ≤18 %	Normal
80HA/20TA	95.4	2.74	SD ≤18 %	
20HA/80TA	88.2	3.11	SD ≤18 %	
50HA/50TA	91.4	6.55	SD ≤18 %	

OD – absolute value.
SD - standard deviation.

the microstructural changes in the films caused by TA acting as a cross-linker and stabilizer for natural polymers, as observed in some of the previous studies [37]. We assume that both polymers (HA and TA) form a cross-linked complex in developed films, where the mechanical properties are the relative result of pre-reactants' properties. Some previous studies have shown that TA contains multiple phenolic groups and can cross-link macromolecules (such as those of hyaluronic acid) by hydrogen, coordination, and hydrophobic bonds [38]. Similar results can be found in literature by other authors. For instance, Gwak et al. observed that the addition of TA to HA-catechol hydrogels improves their mechanical strength [39]. Lee et al. confirmed that the addition of TA results in an increase in mechanical response of polyethylene glycol diglycidyl ether (PEGDE)-crosslinking HA hydrogels [40]. In our research, the 20HA/80TA films had the best mechanical properties. Due to potential application issues, the 80HA/20TA films (with diametrically weak mechanical properties) are not recommended for biomedical applications.

The material applied on the skin should allow for the permeation of water vapor as the appropriate moist environment is one of the most critical factors. It is related to the dressings' ability to remove moisture from the wound into the atmosphere. In in vivo model it was proven that higher WVPR of dressing ensures adequate level of moisture, which results in scar-free healing. Hence, this parameter is useful to determine how the studied material can achieve the balance between a moist wound environment and, at the same time, avoiding the collection of excess exudate that can cause maceration of healthy skin and proneness to infection. Further, it was found that WVPR is strongly related to the porosity and thickness of the applied dressing. Finally, due to the complexity of the wound regeneration process, choosing the appropriate moisture level may be difficult and the water vapor permeation rate is only a helpful indicator that still has some limitations [41,42]. The increasing content of hyaluronic acid in the fabricated films results in the increase in WVPR. Hyaluronic acid is known as a polysaccharide of highly hydrophilic character, so it is able to bind water molecules which are then able to permeate through the film. Such property allows keeping the wound moist and promoting the healing processes.

Hyaluronic acid has been recognized as a polymer with a high ability to bind water [43]. It displays high hydrophilic properties and, thereby, has the ability to swell. However, the consequence of its high hydrophilic character is its low stability in water conditions and its ability to dissolve in water easily [44]. Tannic acid has a weaker ability to swell than hyaluronic acid; however, its addition to hyaluronic acid improves the stability of obtained films. Moreover, the addition of tannic acid provides new properties of hyaluronic acid-based films such as antioxidant activity. The RSA value increases with an increasing concentration of tannic acid in the material. Materials showing antioxidant activity are useful from the biomedical applications viewpoint as they inhibit the free oxygen radicals harmful for human bodies. Materials with antioxidant properties improve the efficiency of medical treatment of wounds and protect the body defects against oxidation stress [45]. Matrix metalloproteinases (MMPs) play an important role in tissue remodeling. Tannic acid has been reported to inhibit MMP-2/−9 activities. Thereby, tannic acid has been recognized as a compound that improves the activity of tissue remodeling as well as wound healing. Chiang et al. [46] explained that the interactions between tannic acid and MMPs including H-bond formation, hydrophobic interactions, and metal–organic coordination bonds. Thereby, tannic acid is a valuable additive which provides antioxidant properties of hyaluronic acid-based materials.

Hyaluronic acid is a well-known biomaterial characterized by excellent biocompatibility [47], while tannic acid has also been previously tested for biocompatibility in a variety of films and scaffolds such as poly(vinly alcohol)/ calcium meta phosphate/tannic acid (PVA/CMP/TA) hydrogel [48], tannic acid (TA)-reinforced methacrylated chitosan (CSMA)/methacrylated silk fibroin (SFMA) hydrogels [49], bacterial cellulose/tannic acid (BC/TA) film [50] or sodium alginate/glycerol/tannic acid (SA/Gly/TA) film [26]. Moreover, both acids are approved by the Food and Drug Administration (FDA) [51]. Hence, it was assumed that the developed films should theoretically be fully biocompatible as well. In our studies, the obtained films were confirmed to be hemocompatible, but only 50HA/50TA was proved to be fully cytocompatible for hFOB cells. Lack of negative influence of the films on human blood is consistent with the literature results. Tannic acid was previously tested as a coating on polyethersulfone (PES) hemodialysis

membranes [52] and hyaluronic acid was used as a wound dressing material for hemostatis [53]. The achieved results of MTT proliferation test show that both 20HA/80TA and 80HA/20TA inhibit the hFOB1.19 cell growth. It may result from a higher release of one of the films' component into the culture medium. On the other hand, the released constituent is not cytotoxic because the LDH release was not elevated under the latter conditions. However, relatively different results were obtained by other authors. For instance, Feng et al. [54] found that the addition of a small amount of TA (5 wt% content) into poly(vinyl alcohol)/carboxymethyl cellulose (PVA/CMC) hydrogels improved cell proliferation. Sharma et al. [26] added TA (30 wt%) into sodium alginate/glycerol (SA/Gly) and also reported a similar positive effect. Moreover, Bai et al. confirmed that the cell proliferation increases with an increase in TA amount added into poly(vinyl alcohol)/collagen (PVA/Col) hydrogels [55]. The differences between our research results and those by other authors may be related to the amount of substances released from both hyaluronic and tannic acid. The above assumption is consistent with the observations of Zhang et al. [56] who found that their composite based on bacterial cellulose/tannic acid also showed cell viability on 60–70 % level and confirmed the association with the TA release. Hence, the most favorable cellular response was observed when the content of the both acids in the 50HA/50TA film was equal. At the same time, all the films are safe to use on the skin as they do not show the irritation effect, as it was also examined with an innovative method involving Reconstructed Human Epidermis.

Bacterial infections are a serious issue for the currently used biomaterials. Therefore, it is extremely important to design materials with their own antibacterial protection. In our research, the developed films showed antibacterial abilities attributable to the use of tannic acid. These polyphenols have previously confirmed bactericidal effectiveness against i.e. *Staphylococcus aureus*, *Klebsiella pneumonia*, *Escherichia coli* and *Helicobacter pylori* [57,58]. Moreover, Shimamura et al. observed that TA efficiently reduces *Staphylococcus aureus* biofilm formation [59]. Our films, combining tannic and hyaluronic acid (80/20, 50/50 and 20/80) maintained their antibacterial properties. These properties are attributed to the presence of phenolic hydroxyl groups which may cause disintegration of the bacterial cell membrane, reduction of enzyme activity, or deprivation of substrates, ions and minerals [60,61]. We found that the tested film have more effective inhibitory effect on *Eschericha coli* (~16 %, 1 h; ~9 %, 2 h; Bacteria Gram-negative) than *Staphylococcus aureus* (~6 %, 1 h; ~6 %, 2 h, ~12 %, 3 h, ~7 %, 4 h; Bacteria Gram-positive). Generally, Gram-negative bacteria have a thin peptidoglycan layer and also an outer lipid membrane, which makes them more resistant to external factors, such as antibiotics [62], which is inconsistent with our results. Also, Briaud et al. confirmed that polyphenols present lower activity against Gram-negative bacteria (tested on *P. aeruginosa*) due to the lack of binding to their walls [63]. The discrepancies may be attributed to the use of different bacteria or a mechanism of TA action different than those assumed by the above-mentioned scientists. Furthermore, we also found that 20HA/80TA films dissolved in broth, which resulted in an increased concentration of the active compounds. The degradation of tannins by bacterial isolates was previously documented in literature and is caused by the hydrolysis of ester bonds by enzymes [64]. We also found that the 50HA/50TA film was the most effective for inhibiting the *Staphylococcus aureus* growth. This may be related to the optimal level of TA in the solution. It was observed earlier that too high concentration of released TA components could cause an increase in the bacterial extracellular matrix and such secretion of polysaccharides may separate bacteria from a reactive tannin or even form the glycocalyx and glycoprotein complex with TA, resulting in a reduction of antibacterial properties [65–67]. Moreover, nanoparticles formed from starch, carboxymethyl chitosan, hyaluronic acid, and tannic acid also showed excellent antibacterial properties and additionally facilitated wound healing acceleration [68].

Based on all the obtained results, we chose the 50HA/50TA film as most suitable for medical applications. This film is characterized by appropriate parameters, such as free surface energy, roughness, mechanical properties, water permeation, and an antioxidant effect as well as full biocompatibility and antibacterial properties against *Staphylococcus aureus* and *Escherichia coli*.

5. Conclusions

Hyaluronic and tannic acid may be mixed to form thin solid films by the solvent evaporation method. The films are characterized by low surface free energy, roughness in the nano scale, antioxidant activity, and also water vapor permeability. All the tested materials were compatible with blood and did not cause an irritation effect. However, only films based on hyaluronic and tannic acid mixed in 50/50 ratio were fully cytocompatible. Thereby, it may be assumed that they have the most suitable properties for the application as wound dressing.

CRediT authorship contribution statement

BKS: Conceptualization, Methodology, Validation, Investigation, Data curation, Visualization, Formal analysis, Writing – original draft, Writing – review & editing, Project Administration; MW: Methodology, Investigation, Data curation, Visualization, Formal analysis, Writing – original draft, Writing – review & editing; AR: Methodology, Formal analysis, Writing – review & editing, Supervision; AM: Methodology, Formal analysis, Writing – review & editing, Supervision; AP: Methodology, Formal analysis; LZ: Methodology, Data curation, Visualization, Formal analysis. MM: Formal analysis, Writing – review & editing, AK: Formal analysis, Writing – review & editing. All authors have read and agreed to the published version of the manuscript.

Declaration of competing interest

The authors declare that they have no known competing financial interests or personal relationships that could have appeared to influence the work reported in this paper.

Data availability

The raw/processed data required to reproduce these findings cannot be shared at this time as the data also forms part of an ongoing study.

Acknowledgements

This research was funded by Nicolaus Copernicus University in Torun (grant number 282/2021 IDUB) (B.K.S.). We wish to express our deep gratitude to Aleksandra Laska for the technical assistance in nanoindentation tests.

Appendix A. Supplementary data

Supplementary data to this article can be found online at https://doi.org/10.1016/j.ijbiomac.2023.128101.

References

[1] R. Bahrami, R. Zibaei, Z. Hashami, S. Hasanvand, F. Garavand, M. Rouhi, S. M. Jafari, R. Mohammadi, Modification and improvement of biodegradable packaging films by cold plasma; a critical review, Crit. Rev. Food Sci. Nutr. 62 (2022) 1936–1950, https://doi.org/10.1080/10408398.2020.1848790.
[2] R. Uppal, G.N. Ramaswamy, C. Arnold, R. Goodband, Y. Wang, Hyaluronic acid nanofiber wound dressing-production, characterization, and in vivo behavior, J. Biomed. Mater. Res. B Appl. Biomater. 97B (2011) 20–29, https://doi.org/10.1002/jbm.b.31776.
[3] K.C. Castro, M.G.N. Campos, L.H.I. Mei, Hyaluronic acid electrospinning: challenges, applications in wound dressings and new perspectives, Int. J. Biol. Macromol. 173 (2021) 251–266, https://doi.org/10.1016/j.ijbiomac.2021.01.100.
[4] F. Garavand, M. Rouhi, S.H. Razavi, I. Cacciotti, R. Mohammadi, Improving the integrity of natural biopolymer films used in food packaging by crosslinking

approach: a review, Int. J. Biol. Macromol. 104 (2017) 687–707, https://doi.org/10.1016/j.ijbiomac.2017.06.093.
[5] P. Singh, P. Baisthakur, O.S. Yemul, Synthesis, characterization and application of crosslinked alginate as green packaging material, Heliyon 6 (2020), e03026, https://doi.org/10.1016/j.heliyon.2019.e03026.
[6] E. Papakonstantinou, M. Roth, G. Karakiulakis, Hyaluronic acid: a key molecule in skin aging, Dermatoendocrinol 4 (2012) 253–258, https://doi.org/10.4161/derm.21923.
[7] S.P. Evanko, T.N. Wight, Intracellular localization of hyaluronan in proliferating cells, J. Histochem. Cytochem. 47 (1999) 1331–1341, https://doi.org/10.1177/002215549904701013.
[8] V. Hascall, Intracellular hyaluronan: a new frontier for inflammation? Biochim. Biophys. Acta Gen. Subj. 1673 (2004) 3–12, https://doi.org/10.1016/j.bbagen.2004.02.013.
[9] G. Weindl, M. Schaller, M. Schäfer-Korting, H.C. Korting, Hyaluronic acid in the treatment and prevention of skin diseases: molecular biological, pharmaceutical and clinical aspects, Skin Pharmacol. Physiol. 17 (2004) 207–213, https://doi.org/10.1159/000080213.
[10] G. Abatangelo, V. Vindigni, G. Avruscio, L. Pandis, P. Brun, Hyaluronic acid: redefining its role, Cells 9 (2020) 1743, https://doi.org/10.3390/cells9071743.
[11] R.D. Price, M.G. Berry, H.A. Navsaria, Hyaluronic acid: the scientific and clinical evidence, J. Plast. Reconstr. Aesthet. Surg. 60 (2007) 1110–1119, https://doi.org/10.1016/j.bjps.2007.03.005.
[12] K.L. Goa, P. Benfield, Hyaluronic acid, Drugs 47 (1994) 536–566, https://doi.org/10.2165/00003495-199447030-00009.
[13] T.C. Laurent, J.R.E. Fraser, Hyaluronan [1], FASEB J. 6 (1992) 2397–2404, https://doi.org/10.1096/fasebj.6.7.1563592.
[14] J.A. Burdick, G.D. Prestwich, Hyaluronic acid hydrogels for biomedical applications, Adv. Mater. 23 (2011) H41–H56, https://doi.org/10.1002/adma.201003963.
[15] H. Ying, J. Zhou, M. Wang, D. Su, Q. Ma, G. Lv, J. Chen, In situ formed collagen-hyaluronic acid hydrogel as biomimetic dressing for promoting spontaneous wound healing, Mater. Sci. Eng. C 101 (2019) 487–498, https://doi.org/10.1016/j.msec.2019.03.093.
[16] S. Grabska, A. Sionkowska, B. Kaczmarek, The physicochemical properties of 3D materials based on hyaluronic acid modified by tannic acid addition, Mol. Cryst. Liq. Cryst. 670 (2018) 90–96, https://doi.org/10.1080/15421406.2018.1542069.
[17] B. Kaczmarek, Tannic acid with antiviral and antibacterial activity as a promising component of biomaterials—a minireview, Materials 13 (2020) 3224, https://doi.org/10.3390/ma13143224.
[18] B. Kaczmarek-Szczepańska, M.M. Sionkowska, O. Mazur, J. Świątczak, M. S. Brzezinska, The role of microorganisms in biodegradation of chitosan/tannic acid materials, Int. J. Biol. Macromol. 184 (2021) 584–592, https://doi.org/10.1016/j.ijbiomac.2021.06.133.
[19] W.A. Arismendi, A.E. Ortiz-Ardila, C.V. Delgado, L. Lugo, L.G. Sequeda-Castañeda, C.A. Celis-Zambrano, Modified tannins and their application in wastewater treatment, Water Sci. Technol. 78 (2018) 1115–1128, https://doi.org/10.2166/wst.2018.336.
[20] S. Khadem, R.J. Marles, Monocyclic phenolic acids; hydroxy- and polyhydroxybenzoic acids: occurrence and recent bioactivity studies, Molecules 15 (2010) 7985–8005, https://doi.org/10.3390/molecules15117985.
[21] J. Xu, Y. Li, Y. Chen, L. Wang, M. Liao, Preparation and characterization of a novel polysialic acid/gelatin composite hydrogels cross-linked by tannic acid to improve wound healing after cesarean section dressing, J. Biomater. Sci. Polym. Ed. 32 (2021) 1927–1943, https://doi.org/10.1080/09205063.2021.1950961.
[22] J. Yang, M. Li, Y. Wang, H. Wu, T. Zhen, L. Xiong, Q. Sun, Double cross-linked chitosan composite films developed with oxidized tannic acid and ferric ions exhibit high strength and excellent water resistance, Biomacromolecules 20 (2019) 801–812, https://doi.org/10.1021/acs.biomac.8b01420.
[23] J. Lee, M. Yeo, W. Kim, Y. Koo, G.H. Kim, Development of a tannic acid cross-linking process for obtaining 3D porous cell-laden collagen structure, Int. J. Biol. Macromol. 110 (2018) 497–503, https://doi.org/10.1016/j.ijbiomac.2017.10.105.
[24] X. Wei, J. Li, B. Li, Multiple steps and critical behaviors of the binding of tannic acid to wheat starch: effect of the concentration of wheat starch and the mass ratio of tannic acid to wheat starch, Food Hydrocoll. 94 (2019) 174–182, https://doi.org/10.1016/j.foodhyd.2019.03.019.
[25] M. Hemshekhar, R.M. Thushara, S. Chandranayaka, L.S. Sherman, K. Kemparaju, K.S. Girish, Emerging roles of hyaluronic acid bioscaffolds in tissue engineering and regenerative medicine, Int. J. Biol. Macromol. 86 (2016) 917–928, https://doi.org/10.1016/j.ijbiomac.2016.02.032.
[26] A. Sharma, C. Verma, S. Mukhopadhyay, A. Gupta, B. Gupta, Development of sodium alginate/glycerol/tannic acid coated cotton as antimicrobial system, Int. J. Biol. Macromol. 216 (2022) 303–311, https://doi.org/10.1016/j.ijbiomac.2022.06.168.
[27] M. Michalska-Sionkowska, B. Kaczmarek, M. Walczak, A. Sionkowska, Antimicrobial activity of new materials based on the blends of collagen/chitosan/hyaluronic acid with gentamicin sulfate addition, Mater. Sci. Eng. C 86 (2018) 103–108, https://doi.org/10.1016/j.msec.2018.01.005.
[28] A. Przekora, The summary of the most important cell-biomaterial interactions that need to be considered during in vitro biocompatibility testing of bone scaffolds for tissue engineering applications, Mater. Sci. Eng. C 97 (2019) 1036–1051, https://doi.org/10.1016/j.msec.2019.01.061.
[29] International Standard for Blood Banks & Blood Transfusion Services, NACO, New Delhi, India, 2007 n.d.
[30] A. Zapata, S. Ramirez-Arcos, A comparative study of McFarland turbidity standards and the densimat photometer to determine bacterial cell density, Curr. Microbiol. 70 (2015) 907–909, https://doi.org/10.1007/s00284-015-0801-2.
[31] M. Muhammad, C. Willems, J. Rodríguez-Fernández, G. Gallego-Ferrer, T. Groth, Synthesis and characterization of oxidized polysaccharides for in situ forming hydrogels, Biomolecules 10 (2020) 1185, https://doi.org/10.3390/biom10081185.
[32] A. Salsabila, A. Pratama, A. Nurrochman, H. Hermawan, A. Barlian, E. Prajatelistia, Preparation of tannic acid/hyaluronic acid coating to improve the corrosion resistance of implant material based on AZ31B magnesium alloy, Metals (Basel) 13 (2023) 494, https://doi.org/10.3390/met13030494.
[33] A. Espina, M.V. Cañamares, Z. Jurašeková, S. Sanchez-Cortes, Analysis of iron complexes of tannic acid and other related polyphenols as revealed by spectroscopic techniques: implications in the identification and characterization of iron gall inks in historical manuscripts, ACS Omega 7 (2022) 27937–27949, https://doi.org/10.1021/acsomega.2c01679.
[34] Z. Zhang, Y. Zhao, X. Luo, S. Feng, L. Wu, Preparation of a heparin-like functionalized tannic acid-coated polyethersulfone ultrafiltration membrane for hemodialysis by a simple surface modification method, Appl. Surf. Sci. 572 (2022), 151440, https://doi.org/10.1016/j.apsusc.2021.151440.
[35] Y. Wang, C.J. Hansen, C.-C. Wu, E.J. Robinette, A.M. Peterson, Effect of surface wettability on the interfacial adhesion of a thermosetting elastomer on glass, RSC Adv. 11 (2021) 31142–31151, https://doi.org/10.1039/D1RA05916E.
[36] W.C. Oliver, G.M. Pharr, An improved technique for determining hardness and elastic modulus using load and displacement sensing indentation experiments, J. Mater. Res. 7 (1992) 1564–1583, https://doi.org/10.1557/JMR.1992.1564.
[37] W.C. Oliver, G.M. Pharr, An improved technique for determining hardness and elastic modulus using load and displacement sensing indentation experiments, J. Mater. Res. 7 (1992) 1564–1583, https://doi.org/10.1557/JMR.1992.1564.
[38] S. Henkelman, G. Rakhorst, J. Blanton, W. van Oeveren, Standardization of incubation conditions for hemolysis testing of biomaterials, Mater. Sci. Eng. C 29 (2009) 1650–1654, https://doi.org/10.1016/j.msec.2009.01.002.
[39] M.A. Gwak, B.M. Hong, J.M. Seok, S.A. Park, W.H. Park, Effect of tannic acid on the mechanical and adhesive properties of catechol-modified hyaluronic acid hydrogels, Int. J. Biol. Macromol. 191 (2021) 699–705, https://doi.org/10.1016/j.ijbiomac.2021.09.123.
[40] H.-Y. Lee, C.-H. Hwang, H.-E. Kim, S.-H. Jeong, Enhancement of bio-stability and mechanical properties of hyaluronic acid hydrogels by tannic acid treatment, Carbohydr. Polym. 186 (2018) 290–298, https://doi.org/10.1016/j.carbpol.2018.01.056.
[41] A. Ahmed, G. Getti, J. Boateng, Medicated multi-targeted alginate-based dressings for potential treatment of mixed bacterial-fungal infections in diabetic foot ulcers, Int. J. Pharm. 606 (2021), 120903, https://doi.org/10.1016/j.ijpharm.2021.120903.
[42] M. Afzali, J.S. Boateng, Composite fish collagen-hyaluronate based lyophilized scaffolds modified with sodium alginate for potential treatment of chronic wounds, Polym. (Basel) 14 (2022) 1550, https://doi.org/10.3390/polym14081550.
[43] J. Zhou, B. Zhang, X. Liu, L. Shi, J. Zhu, D. Wei, J. Zhong, G. Sun, D. He, Facile method to prepare silk fibroin/hyaluronic acid films for vascular endothelial growth factor release, Carbohydr. Polym. 143 (2016) 301–309, https://doi.org/10.1016/j.carbpol.2016.01.023.
[44] J. Li, A. He, C.C. Han, D. Fang, B.S. Hsiao, B. Chu, Electrospinning of hyaluronic acid (HA) and HA/gelatin blends, Macromol. Rapid Commun. 27 (2006) 114–120, https://doi.org/10.1002/marc.200500726.
[45] S. Parham, A.Z. Kharazi, H.R. Bakhsheshi-Rad, H. Nur, A.F. Ismail, S. Sharif, S. RamaKrishna, F. Berto, Antioxidant, antimicrobial and antiviral properties of herbal materials, Antioxidants 9 (2020) 1309, https://doi.org/10.3390/antiox9121309.
[46] Y.-T. Chiang, Y.-B. Xiao, S. Hsu, S.-W. Chang, C.-C. Chou, Molecular interactions of tannic acid and matrix metalloproteinases 2 and 9, Comput. Struct. Biotechnol. J. 21 (2023) 2792–2800, https://doi.org/10.1016/j.csbj.2023.04.011.
[47] M. Dovedytis, Z.J. Liu, S. Bartlett, Hyaluronic acid and its biomedical applications: a review, Eng. Regen. 1 (2020) 102–113, https://doi.org/10.1016/j.engreg.2020.10.001.
[48] S. Nkhwa, L. Iskandar, N. Gurav, S. Deb, Combinatorial design of calcium meta phosphate poly(vinyl alcohol) bone-like biocomposites, J. Mater. Sci. Mater. Med. 29 (2018) 128, https://doi.org/10.1007/s10856-018-6133-6.
[49] X. He, X. Liu, J. Yang, H. Du, N. Chai, Z. Sha, M. Geng, X. Zhou, C. He, Tannic acid-reinforced methacrylated chitosan/methacrylated silk fibroin hydrogels with multifunctionality for accelerating wound healing, Carbohydr. Polym. 247 (2020), 116689, https://doi.org/10.1016/j.carbpol.2020.116689.
[50] S. Gustaite, J. Kazlauske, J. Bobokalonov, S. Perni, V. Dutschk, J. Liesiene, P. Prokopovich, Characterization of cellulose based sponges for wound dressings, Colloids Surf. A Physicochem. Eng. Asp. 480 (2015) 336–342, https://doi.org/10.1016/j.colsurfa.2014.08.022.
[51] S. Parham, A.Z. Kharazi, H.R. Bakhsheshi-Rad, H. Nur, A.F. Ismail, S. Sharif, S. RamaKrishna, F. Berto, Antioxidant, antimicrobial and antiviral properties of herbal materials, Antioxidants 9 (2020) 1309, https://doi.org/10.3390/antiox9121309.
[52] Z. Zhang, Y. Zhao, X. Luo, S. Feng, L. Wu, Preparation of a heparin-like functionalized tannic acid-coated polyethersulfone ultrafiltration membrane for hemodialysis by a simple surface modification method, Appl. Surf. Sci. 572 (2022), 151440, https://doi.org/10.1016/j.apsusc.2021.151440.
[53] M. Hemshekhar, R.M. Thushara, S. Chandranayaka, L.S. Sherman, K. Kemparaju, K.S. Girish, Emerging roles of hyaluronic acid bioscaffolds in tissue engineering

and regenerative medicine, Int. J. Biol. Macromol. 86 (2016) 917–928, https://doi.org/10.1016/j.ijbiomac.2016.02.032.
[54] X. Feng, X. Hou, C. Cui, S. Sun, S. Sadik, S. Wu, F. Zhou, Mechanical and antibacterial properties of tannic acid-encapsulated carboxymethyl chitosan/polyvinyl alcohol hydrogels, Eng. Regen. 2 (2021) 57–62, https://doi.org/10.1016/j.engreg.2021.05.002.
[55] Z. Bai, T. Wang, X. Zheng, Y. Huang, Y. Chen, W. Dan, High strength and bioactivity polyvinyl alcohol/collagen composite hydrogel with tannic acid as cross-linker, Polym. Eng. Sci. 61 (2021) 278–287, https://doi.org/10.1002/pen.25574.
[56] Z.-Y. Zhang, Y. Sun, Y.-D. Zheng, W. He, Y.-Y. Yang, Y.-J. Xie, Z.-X. Feng, K. Qiao, A biocompatible bacterial cellulose/tannic acid composite with antibacterial and anti-biofilm activities for biomedical applications, Mater. Sci. Eng. C 106 (2020), 110249, https://doi.org/10.1016/j.msec.2019.110249.
[57] W. Jing, C. Xiaolan, C. Yu, Q. Feng, Y. Haifeng, Pharmacological effects and mechanisms of tannic acid, Biomed. Pharmacother. 154 (2022), 113561, https://doi.org/10.1016/j.biopha.2022.113561.
[58] F. Heidari, I. Akbarzadeh, D. Nourouzian, A. Mirzaie, H. Bakhshandeh, Optimization and characterization of tannic acid loaded niosomes for enhanced antibacterial and anti-biofilm activities, Adv. Powder Technol. 31 (2020) 4768–4781, https://doi.org/10.1016/j.apt.2020.11.008.
[59] Y. Shimamura, N. Aoki, Y. Sugiyama, T. Tanaka, M. Murata, S. Masuda, Plant-derived polyphenols interact with staphylococcal enterotoxin a and inhibit toxin activity, PloS One 11 (2016), e0157082, https://doi.org/10.1371/journal.pone.0157082.
[60] G. Goel, A.K. Puniya, K. Singh, Tannic acid resistance in ruminal streptococcal isolates, J. Basic Microbiol. 45 (2005) 243–245, https://doi.org/10.1002/jobm.200410517.
[61] J. Davda, V. Labhasetwar, Characterization of nanoparticle uptake by endothelial cells, Int. J. Pharm. 233 (2002) 51–59, https://doi.org/10.1016/S0378-5173(01)00923-1.
[62] P. Briaud, R.K. Carroll, Extracellular vesicle biogenesis and functions in gram-positive bacteria, Infect. Immun. 88 (2020), https://doi.org/10.1128/IAI.00433-20.
[63] Y. Araújo Martins, T. Zeferino Pavan, R. Fonseca Vianna Lopez, Sonodynamic therapy: ultrasound parameters and in vitro experimental configurations, Int. J. Pharm. 610 (2021), 121243, https://doi.org/10.1016/j.ijpharm.2021.121243.
[64] F. Hassan, M.A. Arshad, H.M. Ebeid, M.S. Rehman, M.S. Khan, S. Shahid, C. Yang, Phytogenic additives can modulate rumen microbiome to mediate fermentation kinetics and methanogenesis through exploiting diet–microbe interaction, Front. Vet. Sci. 7 (2020), https://doi.org/10.3389/fvets.2020.575801.
[65] M.A. Gwak, B.M. Hong, W.H. Park, Hyaluronic acid/tannic acid hydrogel sunscreen with excellent anti-UV, antioxidant, and cooling effects, Int. J. Biol. Macromol. 191 (2021) 918–924, https://doi.org/10.1016/j.ijbiomac.2021.09.169.
[66] M. Cipriano-Salazar, S. Rojas-Hernández, J. Olivares-Pérez, R. Jiménez-Guillén, B. Cruz-Lagunas, L.M. Camacho-Díaz, A.E. Ugbogu, Antibacterial activities of tannic acid against isolated ruminal bacteria from sheep, Microb. Pathog. 117 (2018) 255–258, https://doi.org/10.1016/j.micpath.2018.01.045.
[67] J. Chiquette, K.-J. Cheng, J.W. Costerton, L.P. Milligan, Effect of tannins on the digestibility of two isosynthetic strains of birdsfoot trefoil (*Lotus corniculatus* L.) using in vitro and in sacco techniques, Can. J. Anim. Sci. 68 (1988) 751–760, https://doi.org/10.4141/cjas88-084.
[68] N. Li, X. Yang, W. Liu, G. Xi, M. Wang, B. Liang, Z. Ma, Y. Feng, H. Chen, C. Shi, Tannic acid cross-linked polysaccharide-based multifunctional hemostatic microparticles for the regulation of rapid wound healing, Macromol. Biosci. 18 (2018), https://doi.org/10.1002/mabi.201800209.